J Solid State Electrochem (2011) 15:663–673
DOI 10.1007/s10008-010-1110-0

ORIGINAL PAPER

Inhibition of copper corrosion in 3.5% NaCl solutions by a new pyrimidine derivative: electrochemical and computer simulation techniques

K. F. Khaled · Mohamed N. H. Hamed · K. M. Abdel-Azim · N. S. Abdelshafi

Received: 4 April 2010 / Revised: 13 May 2010 / Accepted: 17 May 2010 / Published online: 30 May 2010

Abstract A new pyrimidine heterocyclic derivative, namely 2-ethylthio-4-(*p*-methoxyphenyl)-6-oxo-1,6-dihydropyrimidine-5-carbonitrile (EPD) was prepared and its inhibition performance towards copper corrosion in 3.5% NaCl solutions was studied by potentiodynamic polarization, electrochemical impedance spectroscopy (EIS) and electrochemical frequency modulation (EFM) measurements. Experimental investigations showed that EPD reduces markedly the copper corrosion in 3.5% NaCl solutions. EFM can be used as a rapid and non destructive technique for corrosion rate measurements without prior knowledge of Tafel constants. Monte Carlo simulation technique incorporating molecular mechanics and molecular dynamics can be used to simulate the adsorption of pyrimidine derivative (EPD) on the Cu (111) surface in 3.5% NaCl.

Keywords Copper · EFM · EIS · Polarization · Corrosion · Modeling

K. F. Khaled (✉) · K. M. Abdel-Azim · N. S. Abdelshafi
Electrochemistry Research Laboratory, Chemistry Department,
Faculty of Education, Ain Shams University,
Roxy,
Cairo, Egypt
e-mail: khaledrice2003@yahoo.com

K. F. Khaled
Materials and Corrosion Laboratory, Chemistry Department,
Faculty of Science, Taif University,
Hawiya,
888 Taif, Kingdom of Saudi Arabia

M. N. H. Hamed
Faculty of Education, Chemistry Department,
Ain Shams University,
Roxy,
Cairo, Egypt

Introduction

Copper and its alloys have wide field of applications in industry and technology because they are easily available and economically suitable, though they rank quite high among the construction materials which undergo corrosion at high rates. The corrosion studies given in the literature related to these metals have concentrated mainly on their anodic polarization characteristics. From these studies, it is known that in neutral or nearly neutral pH conditions, highly protective copper oxides or hydroxides can be formed on the metal surface. In the presence of Cl^- ions the formation of such oxide or hydroxide films makes the events much more complex in the corrosion of copper.

The dissolution reactions of copper in chloride solution can be given as below:

$$Cu + Cl^- \rightleftarrows CuCl_{ads} + e^- \quad (1)$$

$$CuCl_{ads} + Cl^- \rightleftarrows CuCl_2^- \quad (2)$$

$$Cu + 2Cl^- \rightleftarrows CuCl_2^- + e^- (slow) \quad (3)$$

Meanwhile, copper oxide and hydroxide can be formed. The cathodic reaction consists of reduction of oxygen:

$$O_2 + 2H_2O + 4e^- \rightleftarrows 4OH^- \quad (4)$$

The insoluble corrosion products forming on the surface may slow down the rate of anodic dissolution and oxygen reduction reactions. It is already known that copper corrosion could occur in chloride solutions, via degradation

of corrosion products, and complex formations with chlorides. It is explained that the rate of anodic dissolution is proportional to the rate of diffusion of $CuCl_2^-$ into the solution, that in low chloride concentration CuCl may form at the beginning and then the dissolution will proceed in the form of $CuCl_2^-$, the presence of insoluble corrosion products on the metal surface will not be able to prevent the reduction of oxygen [1, 2].

One of the most important methods in the protection of copper against corrosion is the use of organic inhibitors. Organic compounds containing polar groups including nitrogen, sulfur, and oxygen [3–15] have been reported to inhibit copper corrosion. The inhibiting action of these organic compounds is usually attributed to their interactions with the copper surface via their adsorption. Polar functional groups are regarded as the reaction center that stabilizes the adsorption process [16]. In general, the adsorption of an inhibitor on a metal surface depends on the nature and the surface charge of the metal, the adsorption mode, its chemical structure and the type of the electrolyte solution [17].

El-Sayed M. Sherif investigated the influence of 2-amino-5-ethylthio-1,3,4-thiadiazole (AETD) on copper corrosion in aerated HCl solution [18] as well as the influence of 2-amino-5- ethylthio-1,3,4-thiadiazole (AETD) [11], 2-amino-5-ethyl-1,3,4-thiadiazole (AETDA) [19] and 5-(phenyl)-4H-1,2,4-triazole-3-thiole (PTAT) [20] in NaCl solution. It is expected that these compounds show high inhibition efficiency since they are heterocyclic compounds containing more donor atoms, besides that they are non-toxic and cheap. AETD, AETDA, and PTAT proved to be good mixed-type copper corrosion inhibitors and the inhibition efficiency increased with concentration.

Substituted uracils are studied as copper corrosion inhibitors in 3% NaCl [21]. These derivatives include: uracil, 5,6-dihydrouracil; 5-amino-uracil; 2-thiouracil; 5-methyl-thiouracil; dithiouracil, so the substituent influence can be estimated. F. Zucchi et al. [22] studied the inhibiting action of tetrazole derivatives in 0.1 M NaCl solution. The following compounds are tested: tetrazole (T), 5-mercapto-1-methyl-tetrazole (5Mc-1Me-T), 5- mercapto(Na salt)-1-methyl-tetrazole (5NaMc-1Me-T), 5-mercapto-1-acetic acid (Na salt)-tetrazole (5Mc-1Ac-T), 5-mercapto-1-phenyl-tetrazole (5Mc-1Ph-T), 5-phenyl-tetrazole (5Ph-T) and 5-amino tetrazole ($5NH_2$-T) in the range of pH from 4 to 8 and at temperatures of 40 and 80°C.

The purpose of the present work is to test the hypothesis that 2-ethylthio-4-(*p*-methoxyphenyl)-6-oxo-1,6-dihydropyrimidine-5-carbonitrile (EPD), which was synthesized in our laboratory, inhibits corrosion of copper when added to stagnant 3.5% NaCl solutions. The study has been carried out by using potentiodynamic polarization, electrochemical impedance spectroscopy, EIS and electrochemical frequency modulation, EFM. The experimental results will be supported by the DFT calculation and molecular dynamics simulations which can provide an interpretation between the electronic and structural properties of the investigated compounds and their experimental results as corrosion inhibitors.

Experimental

Materials and chemicals

Cylindrical rods of copper specimens obtained from Johnson Mattey (Puratronic, 99.999%) were mounted in Teflon. An epoxy resin was used to fill the space between Teflon and copper electrode. The circular cross sectional area of the copper rod exposed to the corrosive medium, used in electrochemical measurements, was (0.28 cm^2). The EPD is added to the 3.5% NaCl at concentrations of 5×10^{-5}, 10^{-4}, 5×10^{-4} and 10^{-3}M. The aggressive environment used was solution of 3.5% NaCl prepared from analytical reagent-grade chemicals. All other chemicals were of AR grade and the solutions were prepared using bidistilled water.

Synthesis of EPD

In this study, a new pyrimidine heterocyclic derivative, namely 2-ethylthio-4-(*p*-methoxyphenyl)-6-oxo-1,6-dihydropyrimidine-5-carbonitrile (EPD) was prepared in our laboratory where a mixture of 2-mercapto-4-(*p*-methoxyphenyl)-6-oxo-1,6-dihydropyrimidine-5-carbonitrile (0.01 mol) and ethyl iodide (0.01 mol) in ethanolic potassium hydroxide solution (prepared by dissolving 0.56 g, 0.01 mole of KOH in 50 ml ethanol) was heated under reflux for 5 h. The reaction mixture was cooled and poured gradually onto crushed ice. The solid obtained was filtered off and recrystallized from ethanol to give EPD as yellow crystals, with yield 83% and m.p. 250°C.

The IR spectrum of compound EPD showed absorption bands at 3131 (NH), 3020 (aromatic-CH), 2933 (aliphatic-CH), 2218 (CN), 1651 (C═O of cyclic amide), 1603 and 1573 cm-1 (C═N and C═C), The ^{1}H NMR spectrum (DMSO-d_6) of which exhibited signals at δ 1.36 (t, 3H, CH_3 of ethylthio group), 3.25 (q, 2H, CH_2 of ethylthio group), 3.89 (s, 3H, OCH_3), 7.12–8.11 (m, 4H, Ar-H), and 8.28 ppm (s, 1H, NH). The structure of EPD was presented in Fig. 1

Electrochemical measurements

The electrochemical measurements were performed in a typical three-compartment glass cell consisted of the copper specimen as working electrode, platinum counter electrode,

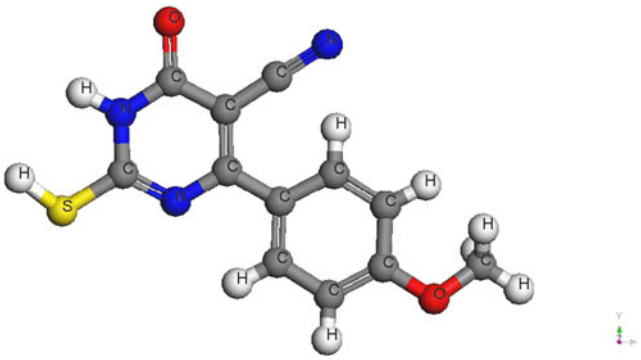

Fig. 1 2-ethylthio-4-(*p*-methoxyphenyl)-6-oxo-1,6-dihydropyrimidine-5-carbonitrile (EPD)

and a saturated calomel electrode as the reference electrode. The counter electrode was separated from the working electrode compartment by fritted glass. The reference electrode was connected to a Luggin capillary to minimize IR drop. Solutions were prepared from bidistilled water of resistivity 13 MΩ cm, the copper electrode was abraded with different grit emery papers size up to 4/0 grade, cleaned with acetone, washed with bidistilled water and finally dried.

Tafel polarization curves were obtained by changing the electrode potential automatically from (−700 to +300 mV_{SCE}) at open circuit potential with a scan rate of 1.0 mV s^{-1}. Impedance measurements were carried out in frequency range from 100 kHz to 40 mHz with an amplitude of 10 mV peak-to-peak using ac signals at open circuit potential. Electrochemical frequency modulation, EFM, was carried out using two frequencies, 2 and 5 Hz. The base frequency was 1 Hz, so the waveform repeats after 1 s. The higher frequency must be at least two times the lower one. The higher frequency must also be sufficiently slow that the charging of the double layer does not contribute to the current response. Often, 10 Hz is a reasonable limit.

The electrode potential was allowed to stabilize 60 min before starting the measurements. All experiments were conducted at 25±1 °C. Measurements were performed using Gamry Instrument Potentiostat/Galvanostat/ZRA. This includes a Gamry framework system based on the ESA400, Gamry applications that include dc105 for dc corrosion measurements, EIS300 for electrochemical impedance spectroscopy and EFM 140 for electrochemical frequency modulation measurements along with a computer for collecting data. Echem Analyst 5.58 software was used for plotting, graphing, and fitting data.

Computational details

The semi-empirical computational methods have been used most successfully in finding correlation between theoretically calculated properties and experimentally determined inhibition efficiency for uniform corrosion [23–33]. The electronic properties of inhibitors, effects of the frontier molecular orbital energies, the differences between lowest unoccupied molecular orbital (LUMO) and highest occupied molecular orbital (HOMO) energies ($E_L - E_H$), electronic charges on reactive centers, dipole moments, and conformation of molecules have been investigated. The geometry optimization process is carried out for the studied EPD compound using an iterative process, in which the atomic coordinates are adjusted until the total energy of a structure is minimized, i.e., it corresponds to a local minimum in the potential energy surface. The forces on the atoms in the EPD molecules are calculated from the potential energy expression and will, therefore, depend on the force field that is selected.

Interaction between EPD and Cu (111) surface was carried out in a simulation box (13.45 Å × 13.45 Å × 43.34 Å) with periodic boundary conditions to model a representative part of the interface devoid of any arbitrary boundary effects. The Cu (111) was first built and relaxed by minimizing its energy using molecular mechanics, then the surface area of Cu (111) was increased and its periodicity is changed by constructing a super cell, and then a vacuum slab with 30 Å thicknesses was built on the Cu (111) surface. The number of layers in the structure was chosen so that the depth of the surface is greater than the non-bond cutoff used in calculation. Using six layers of Cu atoms gives a sufficient depth that the inhibitor molecules will only be involved in non-bond interactions with Cu atoms in the layers of the surface, without increasing the calculation time unreasonably. This structure then converted to have 3D periodicity. As 3D periodic boundary conditions are used, it is important that the size of the vacuum slab is great enough (30 Å) that the non-bond calculations for the adsorbate (EPD molecules) does not interact with the periodic image of the bottom layer of atoms in the surface. After minimizing the Cu (111) surface and EPD molecules, the corrosion system will be built by layer builder to place the inhibitor molecules on Cu (111) surface, and the behaviors of the EPD molecules on the Cu (111) surface were simulated using the COMPASS (condensed phase optimized molecular potentials for atomistic simulation studies) force field.

The Discover molecular dynamics module in Materials Studio 5.0 software from Accelrys Inc. [34] allows selecting a thermodynamic ensemble and the associated parameters, defining simulation time, temperature and pressuring and initiating a dynamics calculation. The molecular dynamics simulations procedures have been described elsewhere [35]. The interaction energy, $E_{Cu\text{-}inhibitor}$, of the Cu (111) surface

with EPD was calculated according to the following equation:

$$E_{\text{Cu-inhibitor}} = E_{\text{complex}} - (E_{\text{Cu-surface}} + E_{\text{inhibitor}}) \quad (5)$$

where E_{complex} is the total energy of the Cu(111) surface together with the adsorbed inhibitor molecule, $E_{\text{Cu-surface}}$ and $E_{\text{inhibitor}}$ are the total energy of the Cu (111) surface and free inhibitor molecule, respectively. The binding energy between EPD and a Cu (111) surfaces was the negative value of the interaction energy [36], as follow:

$$E_{\text{binding}} = -E_{\text{Cu-inhibitor}} \quad (6)$$

Results and discussion

Electrochemical measurements

Polarization curve measurements

The anodic copper dissolution was controlled by both electro-dissolution of copper and diffusion of soluble $CuCl_2^-$ to the bulk solution [37]. Figure 2 shows typical polarization curves for copper in chloride media. The three distinct regions that appeared were the active dissolution region (apparent Tafel region), the active-to-passive transition region, and the limiting current region. In the inhibitor-free solution, the anodic polarization curve of copper (blank curve in Fig. 2) showed a monotonic increase of current with potential until the current reached the maximum value. After this maximum current density value, the current density declined rapidly with potential increase, forming an anodic current peak that was related to CuCl film formation.

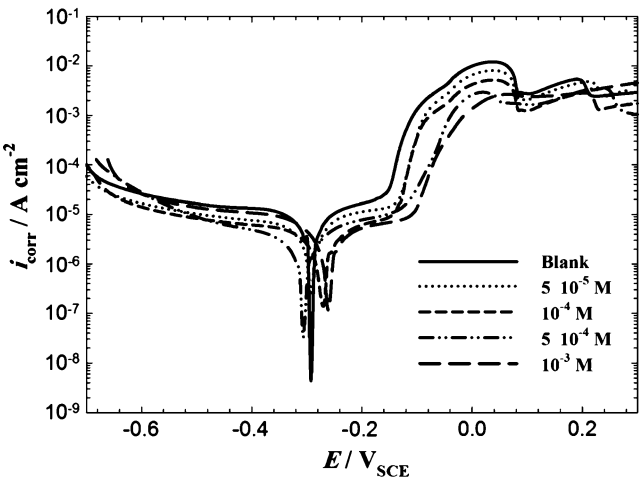

Fig. 2 Anodic and cathodic polarization curves for copper in 3.5% NaCl solutions in the absence and presence of various concentrations of EPD at 25°C±1

In the presence of EPD, both the cathodic and anodic current densities were greatly decreased over a wide potential range from −700 to +300 mV_{SCE}. It was found from Fig. 2 that EPD had a much greater influence on the anodic current in 3.5%NaCl solution than that on the cathodic current.

It is also seen that increasing the EPD concentrations, decreases the cathodic, anodic, and corrosion currents (i_{corr}) and consequently the corrosion rates.

It has been shown that in the Tafel extrapolation method, the use of both the anodic and cathodic Tafel regions is undoubtedly preferred over the use of only one Tafel region [38]. However, the corrosion rate can also be determined by Tafel extrapolation of either the cathodic or anodic polarization curve alone. If only one polarization curve is used, it is generally the cathodic curve which usually produces a longer and better-defined Tafel region. Anodic polarization may sometimes produce concentration effects, due to passivation and dissolution, as well as roughening of the surface which can lead to deviations from Tafel behavior.

The situation here is different; the anodic dissolution of copper in aerated 3.5% NaCl solutions obeys, as previously mentioned, Tafel's law. The anodic curve is, therefore preferred over the cathodic one for evaluation of corrosion currents, i_{corr}, by the Tafel extrapolation method. However, the cathodic polarization curve deviate from the Tafel behavior, exhibiting a limiting diffusion current, may be due to the reduction of dissolved oxygen. Accordingly, there is an uncertainty and source of error in the numerical values of the cathodic Tafel slopes calculated by the software. This is the reason why values of the cathodic Tafel slopes, calculated from the software, are not included here.

Addition of 10^{-3}M of EPD reduces to a great extent the cathodic and anodic currents, i_{corr}. The corresponding electrochemical kinetics parameters such as corrosion potential (E_{corr}), anodic Tafel slopes (β_a) and corrosion current density (i_{corr}), obtained by extrapolation of the Tafel lines are presented in Table 1. The inhibitor efficiency was evaluated from dc measurements using the following equation [39]:

$$\delta_p\% = \left(1 - \frac{i_{\text{corr}}}{i^o_{\text{corr}}}\right) \times 100 \quad (7)$$

where i^o_{corr} and i_{corr} correspond to uninhibited and inhibited current densities, respectively.

Inspection of Table 1, shows that the addition of different concentration of MPD decreases corrosion current densities and increases the inhibition efficiencies $\delta_p\%$.

Electrochemical impedance spectroscopy (EIS)

The other way to evaluate the inhibition effect of EPD is using electrochemical impedance spectroscopy, EIS. An

Table 1 Electrochemical kinetic parameters obtained by potentiodynamic technique for copper in 3.5% NaCl without and with various concentrations of EPD at 25°C±1

	Concentration, (M	i_{corr}, μAcm^{-2}	$-E_{corr}$, mV$_{SCE}$	β_a, mV$_{SCE}$ dec^{-1}	δ_p%
	Blank	11.3	293	227	–
EPD	5×10^{-5}	4.9	293	194	82.7
	10^{-4}	4.2	273	207	85.2
	5×10^{-4}	3.1	306	227	89.1
	10^{-3}	2.4	263	170	91.5

equivalent circuit, such as shown in Fig. 3, was used to consider all the process involved in the electrical response of the system. R_s represents the solution resistance, R_p is the polarization resistance and can be defined also as the charge-transfer resistance, CPE_1 and CPE_2 are constant phase elements (CPEs), R_p' is another polarization resistance and W, is a CPE constant related to Warburg impedance. The different elements were evaluated by a fitting procedure.

Impedance measurements on the copper electrode were performed open to air at the open circuit potential. Figure 4 shows that the Nyquist plots for copper in 3.5% NaCl solution with and without EPD, respectively. The shape of the impedance diagrams of copper in 3.5% NaCl is similar to those found in the literature [40]. The presence of EPD increases the impedance but does not change the other aspects of corrosion mechanism occurred due to its addition. Figure 4 shows the Nyquist plots for copper in 3.5% NaCl without and with different concentrations of MPD. Symbols represent the measured data and solid lines represent the fitting data obtained using the equivalent circuit [19] presented in Fig. 3. The parameters obtained by fitting the experimental data using the equivalent circuit, and the calculated inhibition efficiencies are listed in Table 2. The Nyquist plots presented in Fig. 4 clearly demonstrate that the shapes of these plots for inhibited copper electrode are not substantially different from those of uninhibited electrode. Addition of EPD molecules increases the impedance but does not change other aspects of the electrode behavior. Nyquist spectra presented in Fig. 4 are modeled using an equivalent circuit model similar to the one proposed by several authors [41, 42].

The impedance spectra obtained for copper in 3.5% NaCl contains depressed semicircle with the center under the real axis, such behavior is characteristic for solid electrodes often referred to as frequency dispersion and attributed to the roughness and other inhomogenities of the solid electrode [6, 43].

Deviation of this kind often referred to as frequency dispersion. Therefore, a constant phase element (CPE) instead of a capacitive element is used in Fig. 3 to get a more accurate fit of experimental data sets using generally more complicated equivalent circuits. The impedance, Z, of CPE has the form [44]:

$$Z_{CPE} = [Q(j\omega)^n]^{-1} \quad (8)$$

where Q is the CPE constant, which is a combination of properties related to the surface and electro-active species, $j^2=-1$ the imaginary number, ω the angular frequency and n is a CPE exponent which can be used as a measure of the heterogeneity or roughness of the surface. Depending on the value of n, CPE can represent resistance ($n=0$, $Q=1/R$), capacitance ($n=1$, $Q=C$), inductance ($n=-1$, $Q=1/L$) or CPE constant related to Warburg impedance ($n=0.5$, $Q=W$).

Parameters derived from EIS measurements and inhibition efficiency is given in Table 2. Addition of EPD increases the values of R_p and R_p', and lowers constants of CPE_1 and CPE_2 and this effect is seen to be increased as the concentrations of MPD increase. The CPEs with their n values $1>n>0$ represent double-layer capacitors with some pores [19]. The CPEs decrease upon increase in EPD concentrations, which are expected to cover the charged surfaces and reducing the capacitive effects. This decrease in CPE results from a decrease in local dielectric constant

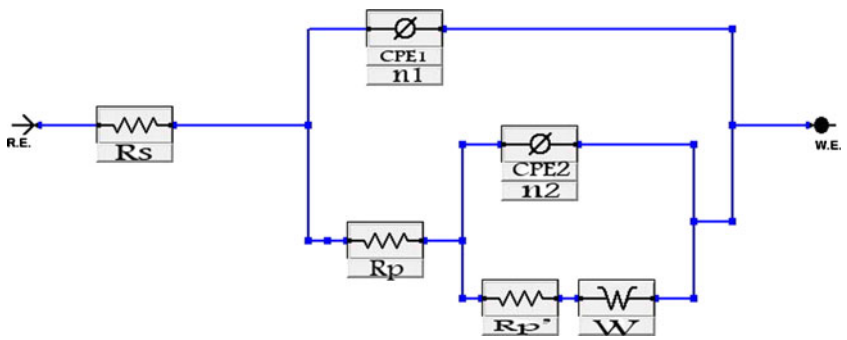

Fig. 3 Equivalent circuit used to model impedance data for copper in 3.5% NaCl solutions in the absence and presence of various concentrations of EPD at 25°C±1

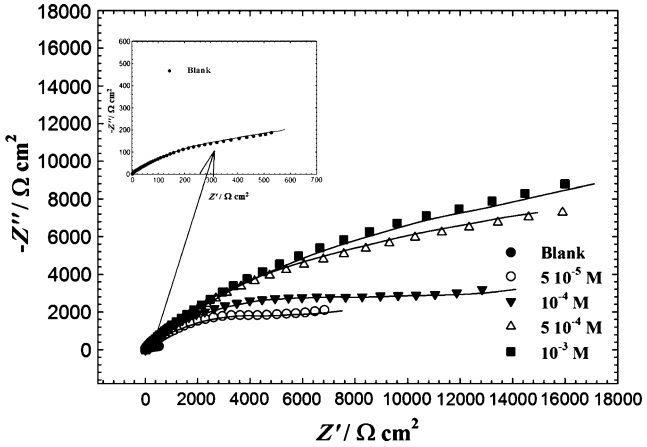

Fig. 4 Nyquist plots for copper in 3.5% NaCl solutions in the absence and presence of various concentrations of EPD at 25°C±1

and/or an increase in the thickness of the double layer, suggested that EPD molecules inhibit the copper corrosion by adsorption at the copper/NaCl interface The semicircles at high frequencies in Fig. 4 are generally associated with the relaxation of electrical double-layer capacitors and the diameters of the high-frequency semicircles can be considered as the charge-transfer resistance (R_{ct}=R_p) [6]. Therefore, the inhibition efficiency, τ_{EIS}% of EPD for the copper electrode can be calculated from the charge-transfer resistance as follows [6]:

$$\tau_{EIS}\% = \left(1 - \frac{R_p^o}{R_p}\right) \times 100 \quad (9)$$

where R_p^o and R_p are the polarization resistances for uninhibited and inhibited solutions, respectively. The CPEs are almost like Warburg impedance with their n values close to 0.5 in presence of EPD [19], which suggests that the electron transfer reaction corresponding to the second semicircle takes place through the surface layer and limits the mass transport (Warburg). The presence of the CPE constant related to Warburg (W) impedance in the circuit confirms also that the mass transport is limited by the surface passive film. The values of copper system could be interpreted as follows: the double-layer capacitance were in the range (1.3 to 0.3 μAcm^{-2}), and simulated as a constant phase element (CPE$_1$) with n_1 value close to 0.8, indicating that the behavior corresponds to a capacitor with some imperfections, such as rough and porous. The first resistance R_p corresponds to the oxidation of the metal, after this oxidation a copper oxide film is formed. This film has a higher resistance due to passive characteristics. The capacity CPE$_2$ of this film was simulated as a constant phase element too, with n_2 value close to 0.5, indicating the porous nature of the film [45]. The presence of EPD on the copper surface, both resistances increase. The first resistance R_p increases as a consequence of the presence of the oxide film, which avoids the penetration of the electrolyte to the copper surface. The second resistance R_p' is the resistance of the EPD film. The capacity of the coated copper electrode is lower than the bare electrode, due to the presence of the film, which decreases the amount of the electrolyte in contact with the copper metal. From the values of R_p and R_p' it is possible to estimate the inhibition efficiency of the EPD on the copper surface as described earlier in Eq. 9.

Electrochemical frequency modulation

The electrochemical frequency modulation (EFM) technique is a new tool for monitoring the electrochemical corrosion. The theory of EFM technique is previously reported [46]. Electrochemical frequency modulation technique has many features [44]. EFM is a nondestructive technique, a rapid test that gives directly values of the corrosion current without a prior knowledge of Tafel constants and has a great strength due to the causality factors, which serve as an internal check on the validity of the EFM measurements.

Figure 5 representing the EFM intermodulation spectra (spectra of current response as a function of frequency) of copper in 3.5% NaCl devoid of and containing various concentrations of EPD at 25°C±1.The inhibition efficiency,

Table 2 Electrochemical parameters calculated from EIS measurements on copper electrode in 3.5% NaCl solutions without and with various concentrations of EPD derivatives 25±1°C using equivalent circuit presented in Fig. 3

Inhibitor		R_s, Ω cm^2	R_p, Ω cm^2	CPE$_1$ Ω^{-1}cm^{-2}s^{n_1}	n_1	R_p'; /Ωcm^2	CPE$_2$ Ω^{-1}cm^{-2}s^{n_2}	n_2	CPE constant related to Warburg impedance Ω^{-1}cm^{-2}s$^{1/2}$	τ_{EIS}%
	Blank	113	733	1.3×10^{-6}	0.89	6.1	13.5×10^{-6}	0.52	20.3×10^{-6}	
EPD	5×10^{-5}	90	4234	0.6×10^{-6}	0.77	12.5	6.3×10^{-6}	0.32	11.4×10^{-6}	83
	10^{-4}	96	4949	0.5×10^{-6}	0.82	13.5	4.3×10^{-6}	0.45	5.6×10^{-6}	86
	5×10^{-4}	93	6694	0.4×10^{-6}	0.79	14.6	3.5×10^{-6}	0.53	3.8×10^{-6}	89
	10^{-3}	90	8674	0.3×10^{-6}	0.81	18.9	2.3×10^{-6}	0.48	2.2×10^{-6}	92

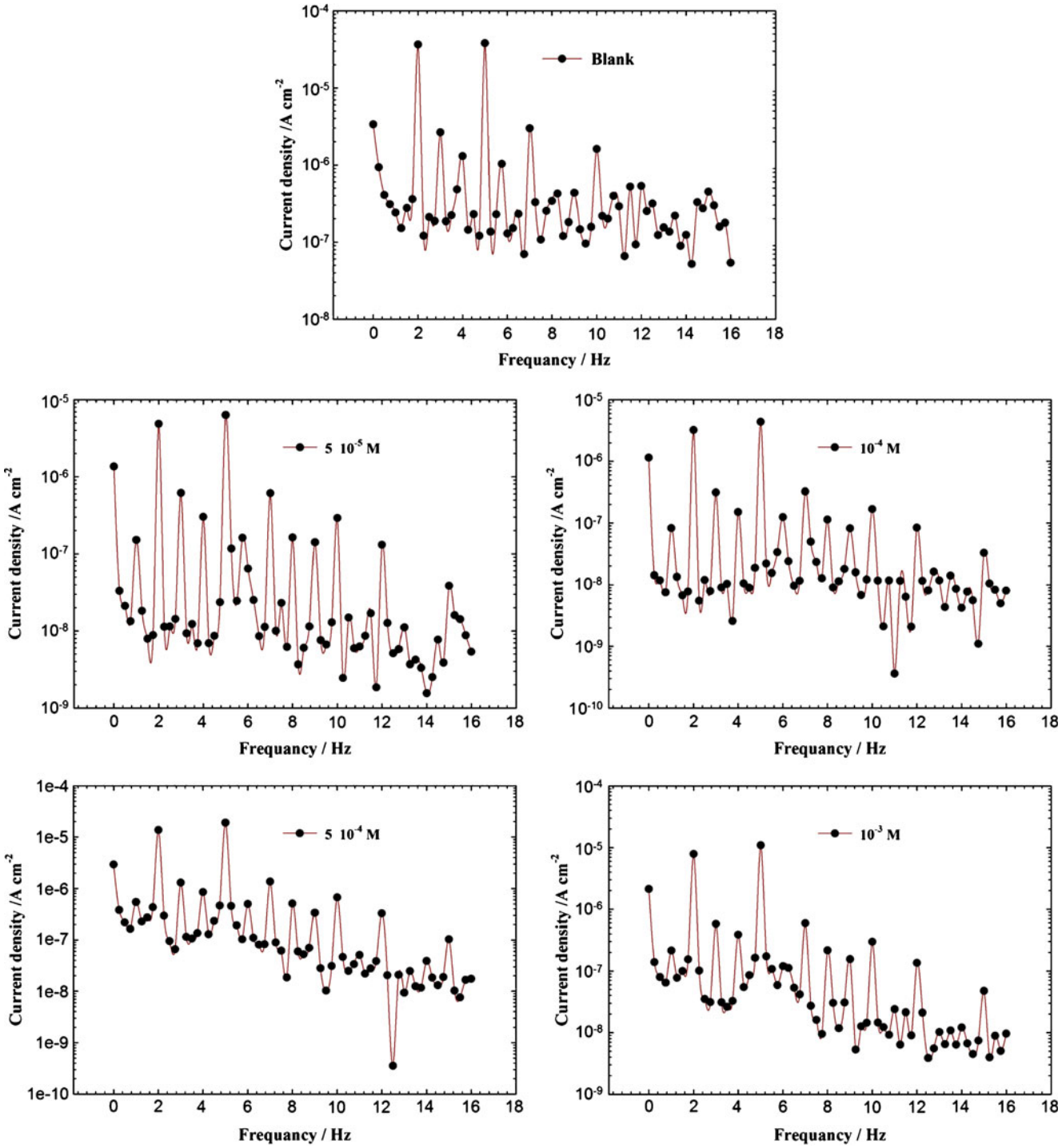

Fig. 5 Intermodulation spectra recorded for copper electrode in 3.5% NaCl solutions in the absence and presence of various concentrations of EPD at 25°C±1

ε_{EFM}%, of EPD was calculated at different concentration using equation presented below:

$$\varepsilon_{EFM}\% = \left(1 - \frac{i_{corr}}{i^{o}_{corr}}\right) \times 100 \qquad (10)$$

where i^{o}_{corr} and i_{corr} are corrosion current density in the absence and presence of MPD compound, respectively.

The calculated electrochemical parameters (i_{corr}, βc, βa, CF-2, CF-3, and ε_{EFM}%) are given in Table 3. As can be seen from Table 3, the corrosion current densities decrease with increase in EPD concentrations. The causality factors in Table 3 indicate that the measured data are of good quality. The standard values for CF-2 and CF-3 are 2.0 and 3.0, respectively. The causality factors are calculated from

Table 3 Electrochemical kinetic parameters obtained by EFM technique for copper in 3.5% NaCl with various concentrations of EPD at 25°C±1

	Concentration, M	i_{corr}, μAcm^{-2}	β_a, mV$_{SCE}$ dec^{-1}	β_c, mV$_{SCE}$ dec^{-1}	C.R, mpy	ε_{EFM}%	CF-2	CF-3
	Blank	71.7	71.7	119.1	117.1		1.9	1.4
EPD	5×10^{-5}	7.7	61.9	106.4	13.2	89.2	1.9	2.3
	10^{-4}	7.0	63.9	91.5	12.6	90.2	1.7	2.8
	5×10^{-4}	4.6	65.7	99.4	10.4	93.6	1.9	1.9
	10^{-3}	3.8	74.4	103.2	8.9	94.6	1.7	2.2

the frequency spectrum of the current response. If the causality factors differ significantly from the theoretical values of 2.0 and 3.0, then it can be deduced that the measurements are influenced by noise. If the causality factors are approximately equal to the predicted values of 2.0 and 3.0, there is a causal relationship between the perturbation signal and the response signal. Then the data are assumed to be reliable [46].

In Table 3, Addition of increasing concentration of EPD to NaCl solutions decreases the corrosion current density (i_{corr}), indicating that EPD inhibits the NaCl corrosion of copper through adsorption. The calculated inhibition efficiency ε_{EFM}% enhances with EPD concentration.

Computational study

Molecular dynamics simulations

Monte Carlo simulation, molecular dynamics were performed on a system comprising EPD molecule and copper surface. EPD is placed on the surface, optimized and then quench molecular dynamics is run. Figure 6 shows the optimization energy curves for the studied molecule (EPD), before putting it on the copper surface. Total energy, average total energy, van der Waals energy, electrostatic energy and intramolecular energy for EPD/copper surface are presented in Fig. 7. The structures of the adsorbate components (EPD) are minimized until they satisfy certain specified criteria. Monte Carlo docking was done on each of the 100 conformations and each of the docked structures was energetically relaxed. The Monte Carlo simulation process tries to find the lowest energy for the whole system [35].

The outputs and descriptors calculated by the Monte Carlo simulation are presented in Table 4. The parameters presented in Table 4 include total energy, in kJ mol^{-1}, of the substrate–adsorbate configuration. The total energy is defined as the sum of the energies of the adsorbate components, the rigid adsorption energy, and the deformation energy. In this study, the substrate energy (copper surface) is taken as zero. Also, adsorption energy in kJ mol^{-1}, reports energy released (or required) when the relaxed adsorbate components are adsorbed on the substrate. The adsorption energy is defined as the sum of the rigid adsorption energy and the deformation energy for the adsorbate components. The rigid adsorption energy, reports the energy, in kJ mol^{-1}, released (or required) when the unrelaxed adsorbate components (i.e., before the geometry optimization step) are adsorbed on the substrate. The deformation energy, reports the energy, in kJ mol^{-1}, released when the adsorbed adsorbate components are relaxed on the substrate surface. Table 4 shows also (dE_{ads}/dN_i), which reports the energy, in kJ mol^{-1}, of substrate–adsorbate configurations where one

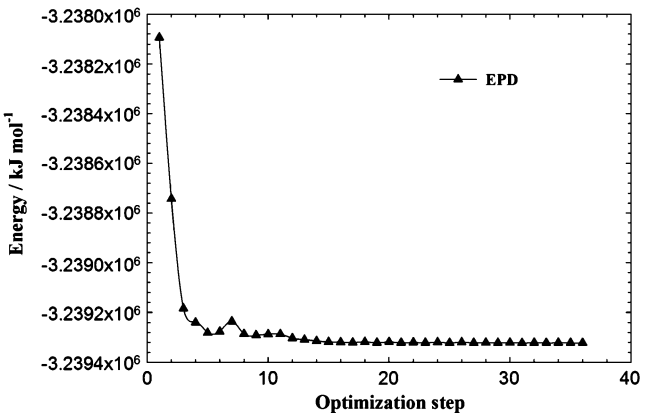

Fig. 6 Optimization energy curves for EPD before putting them on the copper surface

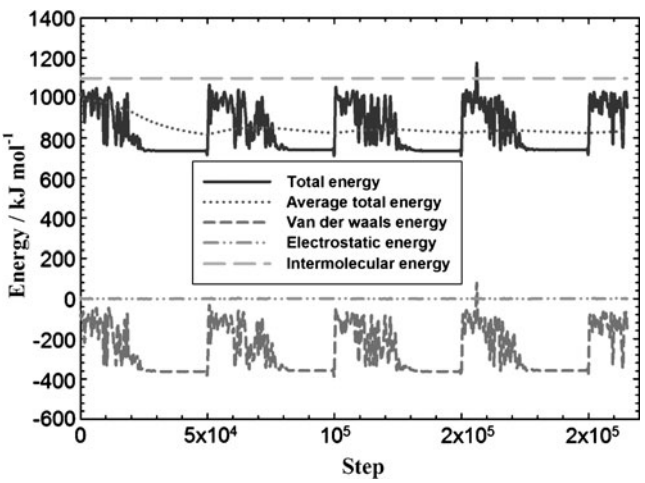

Fig. 7 Total energy distribution for EPD/copper system during energy optimization process

Table 4 Quantum chemical and molecular dynamics parameters derived for EPD calculated with DFT method in aqueous phase

Property	Value
Total energy, kJ mol^{-1}	−294,785.4
μ, D	5.7
E_{HOMO}, kJ mol^{-1}	−840.4
E_{LUMO}, kJ mol^{-1}	−75.3
ΔE, kJ mol^{-1}	769.9
$I = -E_{HOMO}$	840.4
$A = -E_{LUMO}$	75.3
$\chi = (I + A)/2$	457.8
$\eta = (I - A)/2$	382.5
$\Delta N = \frac{\chi_{Cu} - \chi_{inh}}{2(\eta_{Cu} + \eta_{inh})}$	0.007
$E_{Cu\text{-}inhibitor}$, kJ mol^{-1}	−2,111.2
$E_{binding}$, kJ mol^{-1}	2,111.2
Adsorption energy, kJ mol^{-1}	−1,875
Rigid adsorption, energy kJ mol^{-1}	−379.2
Deformation energy, kJ mol^{-1}	−1,495.8
dE_{ad}/dN_i, kJ mol^{-1}	−1,875

of the adsorbate components has been removed. As can be seen from Table 4, EPD gives high adsorption energy during the simulation process. High values of adsorption energy indicate that EPD molecule will give high inhibition efficiency. The best adsorption configuration for the studied compound is shown in Fig. 8. The vertical distance, calculated from molecular dynamics, between the flat EPD molecules and copper surface was about 2.9Å; this result indicates that the interaction between the EPD molecules and the copper surface is enough to inhibit corrosion.

Quantum chemical study

EPD may be adsorbed on the copper surface through three modes according to their molecular structures. The first is as a neutral molecule via chemisorptions mechanism involved sharing electron pair between electronegative atoms and copper/copper oxide surface. In fact, the essence of the adsorption is by coordinating bond through the electronegative atoms donating its electron pair. It is worthy to note that nitrogen, oxygen, sulfur atoms, and unsaturated system in EPD structure have the most probability to form a coordinating bond. The second is through intermolecular force, which is relevant to the dipole of the EPD molecules. The third is through plane-conjugating system constituting the two aromatic rings, which interact through three kinds of mechanism. One is the pyrimidine donating a π electron to metal surface; the second is the pyrimidine accepting the electron from copper surface; while the last are the interactions of hyper conjugations. Quantum chemical calculations were performed in order to confirm the adsorption mechanism. Table 4 shows some of the key quantum chemical parameters were computed using the PM3-SCF method. These are mainly the energies of the highest occupied (E_{HOMO}) and lowest unoccupied (E_{LUMO}) molecular orbitals and total energy (E_{tot}). These quantum chemical parameters were obtained after geometric optimization with respect to the all nuclear coordinates.

The number of transferred electrons (ΔN) was also calculated depending on the quantum chemical method as in the following equation:

$$\Delta N = \frac{\chi_{Cu} - \chi_{inh}}{2(\eta_{Cu} + \eta_{inh})} \tag{11}$$

where χ_{Cu} and χ_{inh} denote the absolute electronegativity of copper and the EPD molecule, respectively; η_{Cu} and η_{inh} denote the absolute hardness of copper and the inhibitor molecule, respectively. These quantities are related to electron affinity (A) and ionization potential (I) which are useful in their ability to help predict chemical behavior [47].

$$\chi = \frac{I + A}{2} \tag{12}$$

$$\eta = \frac{I - A}{2} \tag{13}$$

I and A are related in turn to E_{HOMO} and E_{LUMO}

$$I = -E_{HOMO} \tag{14}$$

$$A = -E_{LUMO} \tag{15}$$

Values of χ and η were calculated by using the values of I and A obtained from quantum chemical calculation. Using a theoretical χ value of 463.12 kJ mol^{-1}according to Pearson's electronegativity scale and η value of 0 kJ mol^{-1}

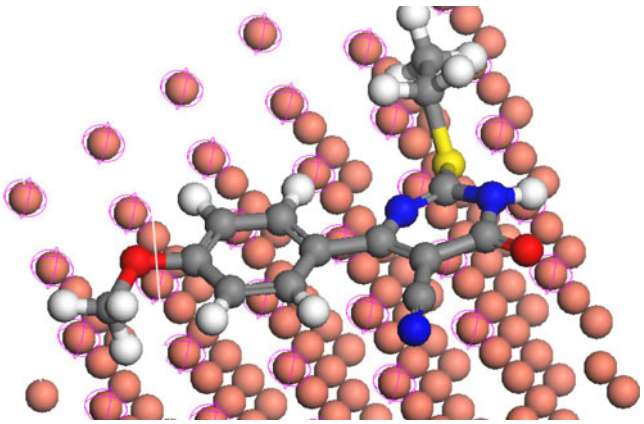

Fig. 8 Most suitable configuration for adsorption of EPD on Cu (111) substrate obtained by Monte Carlo simulation technique

for copper [48], ΔN, the fraction of electrons transferred from inhibitor to the copper surface, was calculated. Values of ΔN showed inhibition effect resulted from electrons donation. Agreeing with Lukovits' study [49], if $\Delta N<3.6$, the inhibition efficiency increased with increasing electron-donating ability at the metal surface. In this study, EPD was the donor of electrons and the copper oxide surface was the acceptor. EPD was bound to the copper oxide surface, and thus formed inhibitive adsorption layer against corrosion.

Inhibition mechanism

Adsorption of EPD can be described by two main types of interactions: physical adsorption and chemisorption. In general, physical adsorption requires the presence of both the electrically charged surface of the metal and charged species in solution. A chemisorption process, on the other hand, involves charge sharing or charge-transfer from the inhibitor molecules to the metal surface to form a coordinate type of a bond. This is possible in the case of a positive as well as a negative charge of the surface. The presence of a transition metal, having vacant, low-energy electron orbitals (Cu^{+} and Cu^{2+}) and of an inhibitor with molecules having relatively loosely bound electrons or hetero-atoms with a lone pair of electrons is necessary [50].

In neutral NaCl solutions, EPD may be adsorbed on the metal surface in the form of neutral molecules involving the displacement of water molecules from the metal surface and sharing of electrons between the nitrogen atoms and the metal surface (chemical adsorption).

Also, the presence of EPD molecules may induce the formation of semiconductive copper oxides as in case of benzotriazoles [51]. This was possibly responsible for the improvement of corrosion resistance.

The type of intermediates that formed on Cu surface in 3.5% NaCl can be explained according to the potential-pH diagram. The presence of Cu_2O may facilitate adsorption via H-bond formation. Another possible mechanism, therefore may be adsorption assisted by hydrogen bond formation between unprotonated N, O, and S atoms in EPD molecule and the oxidized surface (Cu_2O) species. Unprotonated N, O, and S atoms may adsorb by direct chemical adsorption or by hydrogen bonding to a surface oxidized species. The extent of adsorption by the respective modes depends on the nature of the metal surface. The adsorption layer acts as an additional barrier to the corrosive attack and enhances the performance of the passive layer as a result.

The criteria for inhibitor selection can also be inferred from the above considerations. A good inhibitor must have strong affinity for the bare metal atoms. The requirement is different in the presence of the oxide species, a passive oxide film is formed on the electrode surface, where hydrogen bond formation accounts for most of the inhibition action. An effective inhibitor is one that forms hydrogen bonds easily with the oxidized surface. These findings could be further explained on the basis that in presence of dissolved oxygen (the role of dissolved oxygen in oxide formation have been discussed elsewhere [52], where the metal surface is oxidized, the ability of a EPD to provide corrosion inhibition is related to its tendency to form hydrogen bonds with the oxide species on the metal surface. It is quite evident from the chemical structure of EPD molecule that it has NH and SH bonds. These results confirmed the importance of hydrogen bonding in effective corrosion inhibition in presence of oxide species.

Conclusions

Experimental investigations showed that EPD reduces markedly the copper corrosion in 3.5% NaCl solutions, and this reduction in corrosion rates enhances with concentration of this compound. Polarization studies show that this compound acts as mixed-type inhibitor. The results of EIS indicate that the value of CPEs tends to decrease and both charge-transfer resistance and inhibition efficiency tend to increase by increasing the inhibitor concentration. This result can be attributed to increase of the thickness of the electrical double layer. EFM can be used as a rapid and non destructive technique for corrosion rate measurements without prior knowledge of Tafel constants. Molecular dynamic simulations are performed to investigate the adsorption behavior of MPD on copper surface. Monte Carlo simulation technique incorporating molecular mechanics and molecular dynamics can be used to simulate the adsorption of pyrimidine derivative (EPD) on the Cu (111) surface in 3.5% NaCl.

Acknowledgment The authors' gratefully acknowledge the inhibitor preparation carried out by Dr. K. M. El-Mahdy, lecturer of organic chemistry, Chemistry Department, Faculty of Education, Ain Shams University, Roxy, Cairo, Egypt.

References

1. Kabasakaloğlu M, Kıyak T, Şendil O, Asan A (2002) Appl Surf Sci 193:1
2. Kabasakaloğlu M (1991) Corrosion (TR) 3:43
3. Wang C, Chen S, Zhao S (2004) J Electrochem Soc 151:B11
4. Kendig M, Jeanjaquet S (2002) J Electrochem Soc 149:B47
5. Breslin CB, Macdonald DD (1998) Electrochim Acta 44:643
6. Ma H, Chen S, Niu L, Zhao S, Li S, Li D (2002) J Appl Electrochem 32:65
7. Otmaˆciˇc H, Telegdi J, Papp K, Stupnisek-Lisac E (2004) J Appl Electrochem 34:545
8. Zhang D-Q, Gao L-X, Zhou G-D (2004) J Appl Surf Sci 225:287
9. Christy AG, Lowe A, Otieno-Alego V, Stoll M, Webster RD (2004) J Appl Electrochem 34:225

10. Khaled KF, Hackerman N (2004) Electrochem Acta 49:485
11. Sherif EM (2006) J Appl Surf Sci 252:8615
12. Ma HY, Yang C, Yin BS, Li GY, Chen SH, Luo JL (2003) J Appl Surf Sci 218:143
13. Otmaˆciˇc H, Stupnisek-Lisac E (2002) Electrochim Acta 48:985
14. Elmorsi MA, Hassanein AM (1999) Corros Sci 41:2337
15. Scendo M, Poddebniak D, Malyszko J (2003) J Appl Electrochem 33:287
16. Fontana MG, Staehle KW (1970) Advances in corrosion science and technology, vol. 1. Plenum, New York
17. Riggs Jr OL (1973) In: Nathan CC (ed) Corrosion inhibitors, 2nd ed., Houston, TX
18. Sherif EM, Park SM (2006) Electrochim Acta 51:4665
19. Sherif EM, Park SM (2006) Corros Sci 48:4065
20. Sherif EM, Shamy AM, Ramla MM, Nazhawy AOH (2007) Mater Chem and phys 102:231
21. Dafali A, Hammouti B, Mokhlisse R, Kertit S (2003) Corros Sci 45:1619
22. Zucchi F, Trabanelli G, Fonsati M (1996) Corros Sci 38:2019
23. Vosta J, Eliasek J (1971) Corros Sci 11:223
24. Chakrabarti A (1984) Br Corros J 19:124
25. Abdul-Ahad PG, Al-Madfai SHF (1989) Corrosion 45:978
26. Growcock FB (1989) Corrosion 45:1003
27. Costa JM, Lluch JM (1984) Corros Sci 24:929
28. Kutej P, Vosta J, Bartos M (1995) Proc 8th Eur Symp Corros Inhibitors (8SEIC), Ann Univ Ferrara, Italy **10:**896
29. Lukovits I, Kalman E, Baka I, Felhasi I, Teledgi J (1995) Proc 8th Eur Symp Corros Inhibitors (8SEIC), Ann Univ Ferrara, Italy **10:**543
30. Lukovits I, Kostalanyi T, Kalman E, Palinkos G (1999) Conference Corrosion 99, San Antonia, TX, USA 565
31. Awad GH, Asad AN, Abdel Gaber AM, Masud SS (1997) Zashchita Metallov 33:6
32. Bereket G, Ögretir C, Yurt A (571) J Mol Struct (Theochem) 571:139
33. Bereket G, Hür E, Image CÖ (2002) J Mol Struct (Theochem) 578:79
34. Barriga J, Coto B, Fernandez B (2007) Tribol Int 40:960
35. Khaled KF (2009) J Solid Stat Eectrochem 13:1743
36. Mineva T, Parvanov V, Petrov I, Neshev N, Russo N (2001) J Phys Chem A 105:1959
37. Bacarella AL, Griess JC (1973) J Electrochem Soc 120:459
38. McCafferty E (2005) Corros Sci 47:3202
39. Hack HP, Pickering HW (1991) J Electrochem Soc 138:690
40. Khaled KF (2008) Mater Chem and phys 112:104
41. Juttner K, Loranz WJ, Kending MW, Mansfeld F (1988) J Electrochem Soc 135:335
42. Juttner K, Manadhar K, SeiferKraus V, Loranz WJ, Schmidt (1986) Werkst und korr 37:377
43. Pajkossy T (1994) J Electroanal Chem 364:111
44. Abdel-Rehim SS, Khaled KF, Abd-Elshafi NS (2006) Electrochim Acta 51:3269
45. Vera R, Bastidas F, Villarroel M, Oliva A, Molinari A, Ramirez D, Rio R (2008) Corros Sci 50:729
46. Bosch RW, Hubrecht J, Bogaerts WF, Syrett BC (2001) Corrosion 57:60
47. Pearson RG (1986) Proc Nati Acad Sci 83:8440
48. Pearson RG (1988) Inorg Chem 27(1988):734
49. Lukovits I, Kalman E, Zucchi F (2001) Corrosion 57:3
50. Thomas JGN, In Proc 5th Europ Symp on Corrosion Inhibitors, Ann. Univ. Ferrara, Italy, 1980, 1981, pp 453
51. Baba H, Kodama T (1999) Corros Sci 41:1987
52. Amin MA, Khaled KF (2010) Corros Sci 52:1194